Orbital
The electronic journal of chemistry

the electronic journal of chemistry

Short Communication | http://dx.doi.org/10.17807/orbital.v13i1.1574

Green Fluorescent Protein-Mediated Biomineralization of Silver Microparticles

Ma. Monica M. Cabiles [a], Brandon Cyril S. Lira [b], Jose Isagani B. Janairo* [a]

Biomineralization is a bio-inspired technique of creating inorganic nanostructures using peptides or proteins. An important consideration in selecting a biomineralization agent is the overall shape or geometry of the protein since this can influence the properties of the produced nanostructures. The green fluorescent protein (GFP) from the jellyfish *Aequorea victoria* is a promising biomineralization agent due to its distinct structure, characterized by having a barrel-like structure. In this study, silver microparticles (AgMPs) with a diameter of 500 nm were produced through GFP-mediated biomineralization under ambient reaction conditions. In the absence of GFP, aggregated and disordered silver structures were formed. A proposed model to account for the observation involves the formation of GFP networks to which growing silver particles may become adsorbed to. The presented study provides the motivation for the further study of using GFP towards nanostructure synthesis.

Graphical abstract

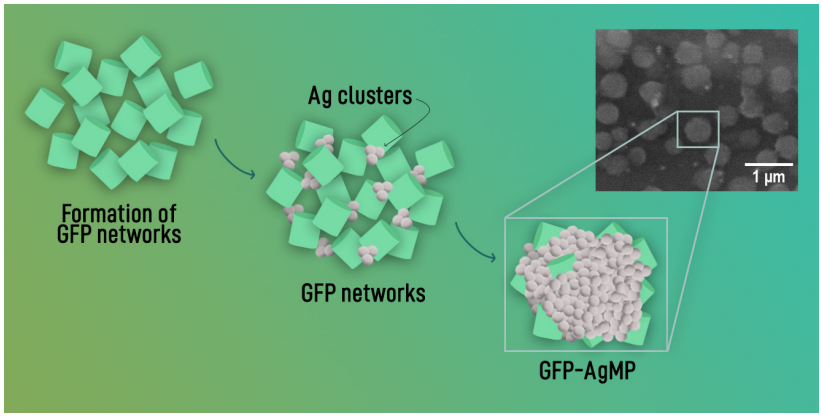

Keywords

Biomimetics
Bionanotechnology
Biomineralization
Inorganic Biochemistry

Article history

Received 25 November 2020
Revised 23 January 2021
Accepted 25 January 2021
Available online 08 March 2021

Editor: Sergio Dovidauskas

1. Introduction

Biomineralization is a biomimetic approach in creating inorganic nanostructures that relies on proteins and peptides. These biomolecules regulate the growth of the nanostructures by acting as templates and capping agents due to their self-assembly and metal coordinating properties [1]. Biomineralization, as a method to create micro and nanomaterials, offers several advantages over traditional bottom-up synthetic methods. Some of these benefits include environment-friendly and non-toxic reaction conditions, and diversity in terms of the types of structures produced since different sequences of peptides and proteins can produce nanomaterials with different properties [2]. A variety of proteins have been documented to be effective for synthesizing nanostructures, such as gelatin [3], the milk protein casein [4], and soy protein [5]. However, an important feature of peptides and proteins that make them attractive biomineralization agents is their overall shape or structure.

The shape or geometry of the biomineralization agent has

[a] Biology Department, De La Salle University, 2401 Taft Avenue, Manila 0922, Philippines. [b] Chemistry Department, De La Salle University, 2401 Taft Avenue, Manila 0922, Philippines. *Corresponding author. E-mail: **jose.isagani.janairo@dlsu.edu.ph**

a significant impact on the structure and properties of the resulting synthesized materials [6]. This strategy in nanomaterial synthesis has led to the creation of nanostructures with improved catalytic activity [6, 7], binding affinity [8], and optical properties [9]. However, controlling the shape and geometry of biomineralization peptides can be tedious and difficult. Biomineralization peptides are relatively short; therefore controlling the way they fold to achieve a certain structure is a challenge. This is often carried out by fusing the peptide to a scaffold that acts as a control element that directs their shape and arrangement. These scaffolds or control elements can be small organic molecules, DNA, short peptide sequences, or proteins [10]. This is in contrast to most proteins which intrinsically possess distinct shapes and geometries which can be immediately utilized for biomineralization. For example, the cage-like protein called ferritin which has a 6 nm cavity was used as a template for nanomaterial synthesis and yielded uniformly sized inorganic nanostructures [11, 12]. The amyloid protein, which is known for its remarkable self-assembly property has also been used as a template for nanomaterials production [13, 14].

A promising protein that has the potential to be an effective template is the green fluorescent protein (GFP) extracted from the jellyfish *Aequorea victoria*. The GFP inherently possesses a barrel-like structure that is 2.4 nm in diameter and 4.2 nm in length [15]. These distinct structural characteristics of the GFP provide a strong motivation to explore its capability as a biomineralization protein. A previous study has also used GFP as a scaffold to which biomineralization peptides were attached to successfully synthesize palladium nanoparticles [16].

In this study, GFP was used as a biomineralization protein to synthesize shape and size-controlled silver particles. The protein's influence on the formation of the synthesized particles was also evaluated.

2. Results and Discussion

The materials produced from the GFP biomineralization are silver microparticles (GFP-AgMP) that follow a normal distribution, with a diameter of 500 ± 115 nm (Figure 1A, inset). These scanning electron microscopy (SEM) images show that the GFP-AgMPs are well dispersed and predominantly spherically shaped (Figure 1, A and B). These observations on the size and morphology of GFP-AgMP are strikingly different from the silver microparticles (AgMPs) synthesized in the absence of the GFP which resulted to be severely aggregated and gave rise to disordered structures (Figure 2, A and B).

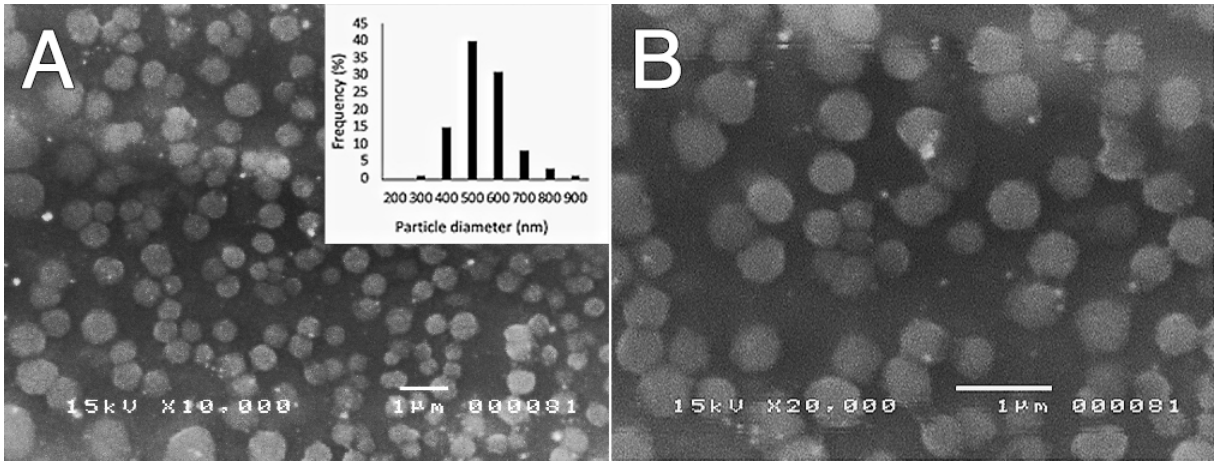

Fig. 1. Morphologies of the GFP-AgMP at (A) 10,000× (inset: particle size distribution histogram) and at (B) 20,000× magnification.

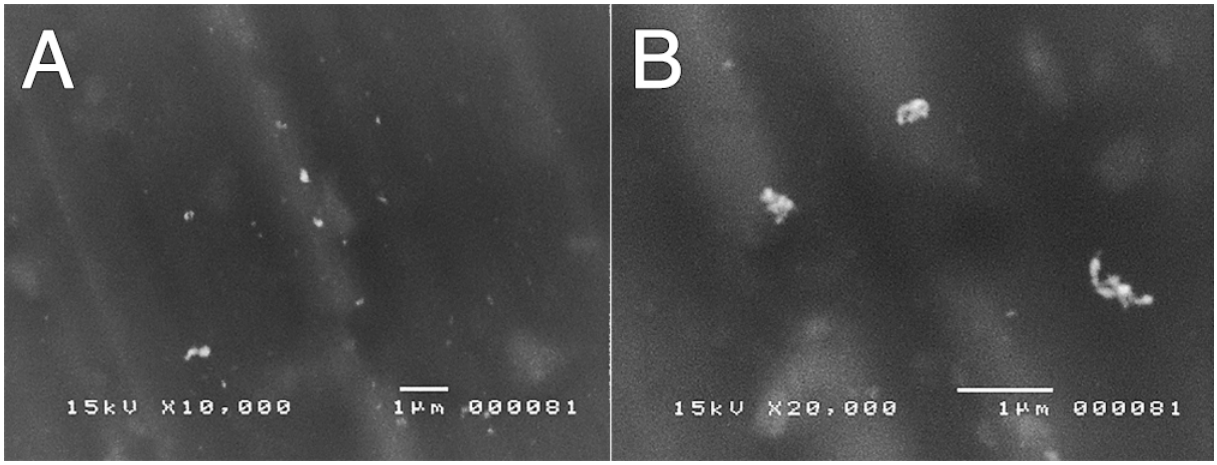

Fig. 2. Morphologies of the AgMP produced in the absence of the protein at (A) 10,000× and at (B) 20,000× magnification.

The absorption spectra for both types of AgMP exhibit a strong absorption maximum at around 400 nm (Figure 3), indicative of surface plasmon resonance that is typical for silver particles. As for the GFP, the strong absorption peak at 400 nm, and a slightly weaker absorption at 480 nm are characteristic for this fluorescent protein [17].

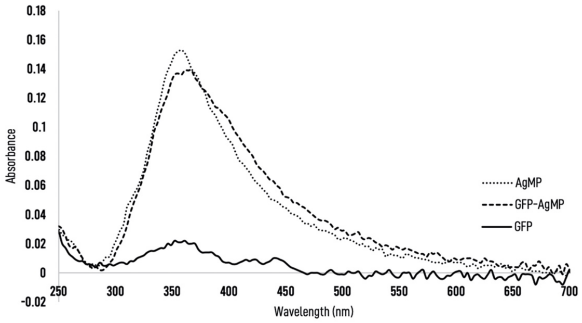

Fig. 3. UV-Vis absorption spectra of AgMP (dotted line), GFP-AgMP (dashed line), GFP (solid line).

The obtained results indicate the effect of GFP on the size and morphology of AgMP during formation. The GFP may serve as nucleation sites for small silver clusters during reduction, wherein the formation of the GFP networks guide the growth of the microparticle. This model is supported by the FTIR analyses which indicate the interaction of GFP with the AgMP.

The FTIR spectra of the GFP and GFP-AgMP are shown in Figure 4. Both of them exhibited peaks at 3354 cm^{-1}, which may be accounted for the presence of the hydroxyl (OH) groups from the water, and the phenolic groups that are present.

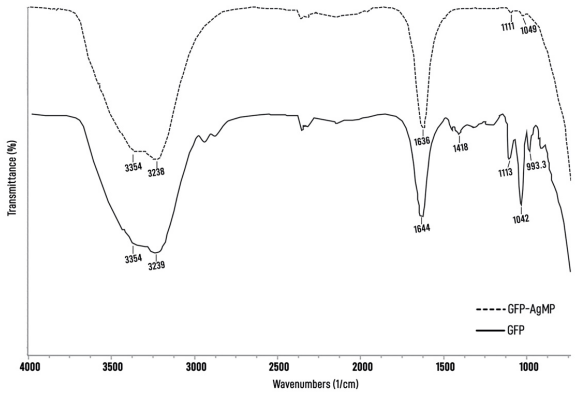

Fig. 4. FTIR spectra for GFP-AgMP (dashed line) and GFP (solid line).

The peak at around 3239 cm^{-1} and 3238 cm^{-1} for GFP and GFP-AgMP, respectively, may be attributed to overlapping N-H stretching vibrations which belong to the amino groups in proteins [18].

The amide I and amide II IR regions are often used to qualitatively assess changes in the protein conformation. In the spectra, the peak occurred at 1644 cm^{-1} for GFP belongs to the amide I band which is related to the carbonyl (C=O) stretching vibration [19]. Particularly, the presence of the amide I band indicates that the protein is in the secondary structure. This peak is also present in GFP-AgMP but at a slightly lower wavenumber at 1636 cm^{-1}. This slight shift to a lower wavenumber can be accounted for a conformational change, which occurred in the secondary structure of the GFP [20] and is associated with its adsorption onto the AgMPs [21-23]. The interaction of the protein to the AgMPs can be attributed to the formation of covalent bonds to the amino groups and the cysteine residues, and through electrostatic interactions to the carboxyl group [24].

For the GFP, a small peak at 1418 cm^{-1} is attributed to the amide II band from the N-H bending and the C-N stretching vibrations [24]. However, in the GFP-AgMP, peaks around this area are absent which might be due to the occurrence of a conformational change in the protein.

Due to the dilution of the GFP, the small peaks appearing at 1113 cm^{-1} and 993.3 cm^{-1} may be from to the splitting of a supposedly very sharp signal at 1042 cm^{-1}, which can be attributed to the carboxylate group (COO^-) of the protein [21, 25]. Similarly, for the GFP-AgMP, small and weak signals for the COO- group are observed at 1111 cm^{-1} and 1047 cm^{-1}.

The formation of the GFP networks (Figure 5) further supports the proposed model of GFP-mediated biomineralization. The shape, size, surface hydrophobicity, and surface charge of the protein are known to contribute to the self-assembly capability of GFP [26].

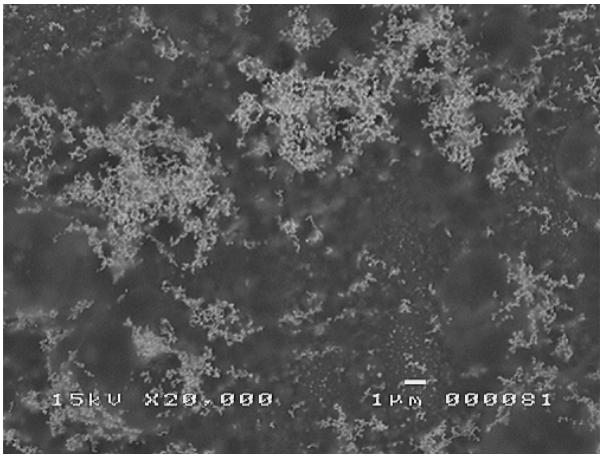

Fig. 5. SEM image of the GFP networks at 20,000× magnification.

Taken together, a model is herein proposed in an attempt to explain silver biomineralization by GFP (Figure 6). In the first stage, GFP forms networks via non-covalent interactions. After the addition of silver ions and reduction, silver clusters are adsorbed with the GFP. Since there is an abundant excess of silver compared with the protein, silver agglomeration continues wherein the GFP remains to be bound to the silver particles in which this occurrence may have an influence on regulating the size and shape of the continuously growing particle.

Silver is one of the most common biomineralized inorganic material, and the most common product of this process is in the form of silver nanoparticles (AgNPs). However, producing silver microparticles (AgMPs) is also valuable and provides advantages in different applications.

In its micro or nanoscale, silver particles are an effective antibacterial agent. One emerging concern is that these silver particles may also pose a threat to humans, as it is known to be toxic to microorganisms due to its small size. In mice, it was found out that both AgNPs and AgMPs are cytotoxic and cause apoptosis, but the damage is more widespread from the AgNPs due to its smaller size. These AgNPs can in fact be distributed from the bloodstream into the vital organs. Meanwhile, AgMPs could not even enter the bloodstream [27-29]. Interestingly, when tested in human red blood cells, AgNPs promote the increase of the blood's procoagulant activity but not with AgMPs [30]. AgMPs were also found to provide steady and greater silver ion release compared to AgNPs, which means that its antibacterial effect would last longer [31]. As a thermal conductor, AgMPs showed superior

thermal conductivity over AgNPs due to its larger size. AgNPs also tend to agglomerate which made them inferior to AgMPs [32]. Thus, the presented method of producing uniformly shaped and sized AgMPs has promising applications in different areas.

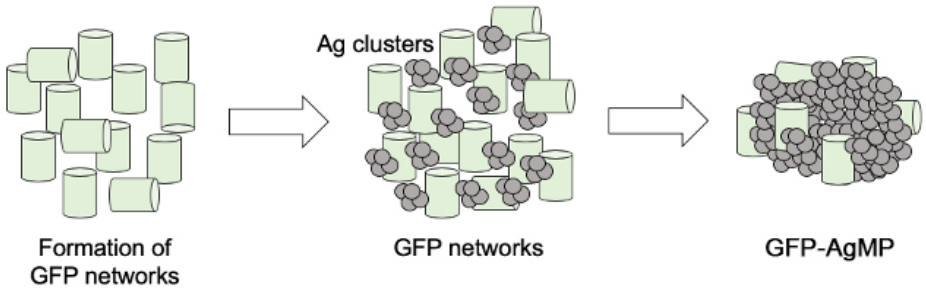

Fig. 6. Proposed model for GFP-mediated silver biomineralization. The cylinders represent the GFP while the spheres represent silver microparticles.

Overall, these results present a simple approach in AgMP synthesis. Moreover, several advantages of GFP-mediated biomineralization include a one-pot and benign reaction setup, and only a small amount of GFP is needed to control AgMP formation. The present approach is also more straightforward and convenient since GFP is utilized as the main biomineralization agent to produce these microparticles.

3. Material and Methods

The GFP-mediated biomineralization of AgMP was conducted by mixing $AgNO_3$ (Sigma-Aldrich) with GFP (E. coli-expressed, N-terminal histidine-tagged green fluorescent protein diluted in PBS containing 20% glycerol from Merck-Millipore) in distilled water to achieve a final concentration of 25 mM for the metal salt and 2 μM for the protein, at pH 7.4. Metal reduction was carried out through the addition of 75 mM of $NaBH_4$ (Sigma-Aldrich) and was allowed to proceed for 30 minutes. For the control experiment, the same reaction conditions were repeated but in the absence of GFP.

The morphology of the produced AgMPs was evaluated through a JEOL JSM-5310 scanning electron microscope. For the GFP-AgMP and the AgMP, the samples were prepared by placing 20 μL of the onto a piece of aluminum foil and then air dried. After air drying, the foil containing sample was then analyzed. The diameter of 100 particles was manually measured using ImageJ [33] and served as the basis for reporting the mean particle diameter. For the SEM analysis of the GFP alone, the dried sample was sputter-coated with gold prior to microscopy.

The absorption spectra of each samples were analyzed using a Thermo Fisher NanoDrop™ 8000 Spectrophotometer at a path length of 1 mm by dropping 1μL aliquots of each samples, as is, on the measurement surface.

FTIR was carried out through attenuated total reflectance (ATR) using a Shimadzu IRAffinity-1S FTIR spectrometer with a QATR-10 diamond crystal-equipped attachment.

4. Conclusions

In summary, predominantly spherically shaped silver microparticles with a uniform size distribution were synthesized using GFP as the biomineralization protein. The effect of the GFP on silver microparticle synthesis was clearly observed, suggesting direct participation during the formation process. The presented method is attractive since it is a one-pot setup, conducted in ambient conditions, and only requires a small amount of GFP. The presented results provide the motivation for further analysis of using GFP to perform controlled inorganic micro and nanoparticle synthesis.

Author Contributions

MMMC: Investigation, Methodology, Writing – original draft; BCSL: Formal analysis, Visualization, Writing – original draft, Writing – review and editing; JIBJ: Conceptualization, Methodology, Supervision, Writing – review and editing

References and Notes

[1] Janairo, J. I. B. Peptide-Mediated Biomineralization, Singapore: Springer, 2016. [Crossref]

[2] Chakraborty, I.; Feliu, N.; Roy, S.; Dawson, K.; Parak, W. J. *Bioconjug. Chem.* **2018**, *29*, 1261. [Crossref]

[3] Liu, Y.; Liu, X.; Wang, X. *Nanoscale Res. Lett.* **2011**, *6*, 1. [Crossef]

[4] Ashraf, S.; Abbasi, A. Z.; Pfeiffer, C.; Hussain, S. Z.; Khalid, Z. M.; Gil, P. R.; Parak, W. J.; Hussain, I. *Colloid Surface B.* **2013**, *102*, 511. [Crossref]

[5] Abdelgawad, A. M.; El-Naggar, M. E.; Eisa, W. H.; Rojas, O. J. *J. Clean. Prod.* **2017**, *144*, 501. [Crossref]

[6] Janairo, J. I. B.; Sakaguchi, T.; Hara, K.; Fukuoka, A.; Sakaguchi, K. *Chem. Commun. (Camb).* **2014**, *50*, 9259. [Crossref]

[7] Song, C.; Wang, Y.; Rosi, N. L. *Angew. Chemie - Int. Ed.* **2013**, *52*, 3993. [Crossref]

[8] Sakaguchi, T.; Janairo, J. I. B.; Lussier-Price, M.; Wada, J.; Omichinski, J. G.; Sakaguchi, K. *Sci. Rep.* **2017**, *7*, 1400. [Crossref]

[9] Song, C.; Blaber, M. G.; Zhao, G.; Zhang, P.; Fry, H. C.; Schatz, G. C.; Rosi, N. L. *Nano Lett.* **2013**, *13*, 3256. [Crossref]

[10] Janairo, J. I. B.; Sakaguchi, T.; Mine, K.; Kamada, R.; Sakaguchi, K. *Protein Pept. Lett.* **2018**, *25*, 4. [Crossref]

[11] Yamashita, I. *Thin Solid Films* **2001**, *393*, 12. [Crossref]

[12] Hosein, H. A.; Strongin, D. R.; Allen, M.; Douglas, T. *Langmuir* **2004**, *20*, 10283. [Crossref]

[13] Nyström, G.; Fernández-Ronco, M. P.; Bolisetty, S.; Mazzotti, M.; Mezzenga, R. *Adv. Mater.* **2016**, *28*, 472. [Crossref]

[14] Malisauskas, M.; Meksys, R.; Morozova-Roche, L. A. *Biotechnol. Prog.* **2008**, *24*, 1166. [Crossref]

[15] Orm, M.; Cubitt, A. B.; Kallio, K.; Gross, L. A.; Tsien, R. Y.; Remington, S. J. *Science* **1996**, *273*, 1392. [Crossref]

[16] Mosleh, I.; Benamara, M.; Greenlee, L.; Beyzavi, M.H.; Beitle, R. *Mater. Lett.* **2019**, *252*, 68. [Crossref]

[17] Morise, H.; Shimomura, O.; Johnson, F. H.; Winant, J. *Biochemistry* **1974**, *13*, 2656. [Crossref]

[18] Othman, A. M.; Elsayed, M. A.; Al-Balakocy, N. G.; Hassan, M. M.; Elshafei, A. M. *J. Genet. Eng. Biotechnol.* **2019**, *17*, 8. [Crossref]

[19] Roach, P.; Farrar, D.; Perry, C. C. *J. Am. Chem. Soc.* **2005**, *127*, 8168. [Crossref]

[20] Lu, D.; Zhang, C.; Fan, L.; Wu, H.; Shuang, S.; Dong, C. *Anal. Methods* **2013,** *5*, 5522. [Crossref]

[21] Espiritu, R. A.; Rebustillo, P. B. C. R. *Bionanoscience* **2017**, *7*, 501. [Crossref]

[22] Zhong, Y.; Zhu, J.; Wang, Q.; He, Y.; Ge, Y.; Song, C. *Microchim. Acta* **2014**, *182*, 909. [Crossref]

[23] Yata, V. K.; Ghosh, S. S. *Mater. Lett.* **2012**, *73*, 209. [Crossref]

[24] Ballottin, D.; Fulaz, S.; Souza, M. L.; Corio, P.; Rodrigues, A. G.; Souza, A. O.; Gaspari, P. M.; Gomes, A. F.; Gozzo, F.; Tasic, L. *Nanoscale Res. Lett.* **2019**, *11*, 1. [Crossref]

[25] Suganya, K. U.; Govindaraju, K.; Kumar, V. G.; Dhas, T. S.; Karthick, V.; Singaravelu, G.; Elanchezhiyan, M. *Mater. Sci. Eng. C* **2015**, *47*, 351. [Crossref]

[26] Lam, C.N.; Kim, M.; Thomas, C.S.; Chang, D.; Sanoja, G.E.; Okwara, C.U.; Olsen, B.D. *Biomacromolecules* **2014**, *15*, 1248. [Crossref]

[27] Wei, L.; Tang, J.; Zhang, Z.; Chen, Y.; Zhou, G.; Xi, T. *Biomed. Mater.* **2010**, *5*, 44. [Crossref]

[28] Cha, K.; Hong, H.W.; Choi, Y.G.; Lee, M.J.; Park, J.H.; Chae, H.K.; Ryu, G.; Myung, H. *Biotechnol. Lett.* **2008**, *30*, 1893. [Crossref]

[29] Tang, J.; Xiong, L.; Wang, S.; Wang, J.; Liu, L.; Li, J.; Yuan, F; Xi, T. *J. Nanosci. Nanotechnol.* **2009**, *9*, 4924. [Crossref]

[30] Bian, Y.; Kim, K.; Ngo, T.; Kim, I.; Bae, O.-N.; Lim, K. M.; Chung, J. H. *Part. Fibre Toxicol.* **2019**, *16*, 1. [Crossref]

[31] Mohiti-Asli, M.; Pourdeyhimi, B.; Loboa, E. G. *Tissue Eng., Part C* **2014**, *20*, 790. [Crossref]

[32] Zulkarnain, M.; Fadzil, M. A.; Mariatti, M.; Azid, I. A. *J. Electron. Mater.* **2017**, *46*, 6727. [Crossref]

[33] Rueden, C. T.; Schindelin, J.; Hiner, M. C.; DeZonia, B. E.; Walter, A. E.; Arena, E. T.; Eliceiri, K. W. *BMC Bioinf.* **2017**, *18*, 529. [Crossref]

How to cite this article

Cabiles, M. M.; Lira, B. C. S.; Janairo, J. I. *Orbital: Electron. J. Chem.* **2021**, *13*, 85.
http://dx.doi.org/10.17807/orbital.v13i1.1574